

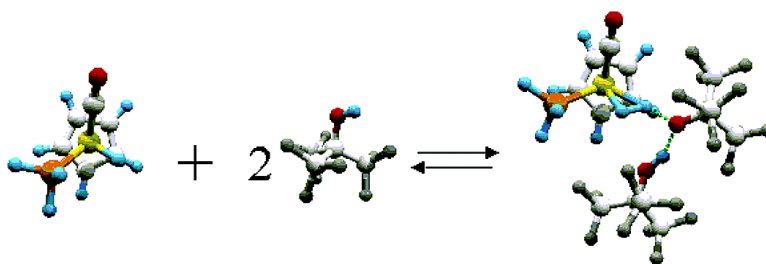
Article

Influence of Media and Homoconjugate Pairing on Transition Metal Hydride Protonation. An IR and DFT Study on Proton Transfer to CpRuH(CO)(PCy)

Natalia V. Belkova, Maria Besora, Lina M. Epstein, Agust Lleds, Feliu Maseras, and Elena S. Shubina

J. Am. Chem. Soc., **2003**, 125 (25), 7715-7725 • DOI: 10.1021/ja029712a • Publication Date (Web): 03 June 2003

Downloaded from <http://pubs.acs.org> on March 29, 2009



More About This Article

Additional resources and features associated with this article are available within the HTML version:

- Supporting Information
- Links to the 7 articles that cite this article, as of the time of this article download
- Access to high resolution figures
- Links to articles and content related to this article
- Copyright permission to reproduce figures and/or text from this article

[View the Full Text HTML](#)



ACS Publications
 High quality. High impact.

Influence of Media and Homoconjugate Pairing on Transition Metal Hydride Protonation. An IR and DFT Study on Proton Transfer to CpRuH(CO)(PCy₃)

Natalia V. Belkova,[†] Maria Besora,[‡] Lina M. Epstein,[†] Agustí Lledós,^{*,‡}
Feliu Maseras,[‡] and Elena S. Shubina^{*,†}

Contribution from A. N. Nesmeyanov Institute of Organoelement Compounds, 28 Vavilov Street, 119991 Moscow, Russia, and Departament de Química, Edifici Cn, Universitat Autònoma de Barcelona, 08193 Bellaterra, Spain

Received December 12, 2002; E-mail: agusti@klington.uab.es

Abstract: The interaction of the ruthenium hydride complex CpRuH(CO)(PCy₃) (**1**) with proton donors HOR of different strength was studied in hexane and compared with data in dichloromethane. The formation of dihydrogen-bonded complexes (**2**) and ion pairs stabilized by hydrogen bonds between the dihydrogen ligand and the anion (**3**) was observed. Kinetics of the interconversion from **2** to **3** was followed at different (CF₃)₃COH concentrations between 200 and 240 K. The activation enthalpy and entropy values for proton transfer from the dihydrogen-bonded complex **2** to the (η²-H₂)-complex **3** (ΔH[‡] = 11.0 ± 0.5 kcal/mol and ΔS[‡] = -19 ± 3 eu) were obtained for the first time. The results of the DFT study of the proton transfer process, taking CF₃COOH and (CF₃)₃COH as a proton donors and introducing solvent effects in the calculation with the PCM method, are presented. The role of homoconjugate pairs [ROHOR]⁻ in the protonation is analyzed by means of the inclusion of an additional ROH molecule in the calculations. The formation of the free cationic complex [CpRu(CO)(PCy₃)(η²-H₂)]⁺ is driven by the formation of the homoconjugated anionic complex [ROHOR]⁻. Solvent polarity plays a significant role stabilizing the charged species formed in the process. The theoretical study also accounts for the dihydrogen release and production of CpRu(OR)(CO)(PCy₃), observed at temperatures above 250 K.

Introduction

In recent years the formation of “unconventional” intramolecular and intermolecular hydrogen bonds involving the hydride ligand as a proton acceptor has been reported.¹ This nonclassical bonding, also called dihydrogen bond, seems to have an activating effect on the metal hydride toward H/D exchange and possibly also toward catalytic hydrogenation.² The idea that these H···H hydrogen-bonded complexes constitute important intermediates of transition metal hydride protonation has been subsequently proposed in a number of works^{3,4} and afterward found its experimental confirmation.^{5,6} For example, the ap-

plication of IR and/or NMR methods in a wide range of temperatures allowed the establishment of the existence of a slow equilibrium between M-H···H-OR and [M-(η²-H₂)]⁺[OR]⁻ species in the case of RuH₂(dppm)₂,⁵ {MeC(CH₂PPh₂)₃}-Re(CO)₂H,⁶ and Cp*Ru(PCy₃)H₃.⁷ In the latter study, where NMR experiments were performed using both toluene and a liquefied Freon mixture CDF₂Cl/CDF₃ (2:1) as solvents, it was realized that protonation takes place if the solvent polarity is large enough. Interestingly, both the Freon mixture and CH₂-Cl₂ possess similar dielectric constants which increase drastically by lowering the temperature. As a consequence, protonation occurs at low temperatures as a solvent-assisted process in contrast to nonpolar toluene, where only the M-H···H-OR complex was observed.⁷

The above-mentioned studies of MH···HOR complexes fit well into the received concept of proton transfer mechanism where the dihydrogen bond formation is the first stage. Usually, in the second stage the hydrogen-bonded complex is converted into an ion pair, leading finally to free ions. In case of transition metal hydrides the process can be visualized as shown in

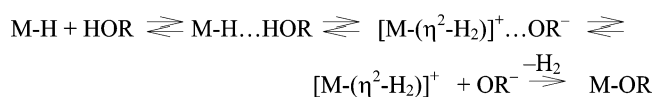
[†] A. N. Nesmeyanov Institute of Organoelement Compounds.

[‡] Universitat Autònoma de Barcelona.

- (1) For reviews on the dihydrogen bonding see: (a) Crabtree, R. H.; Siegbahn, P. E. M.; Eisenstein, O.; Rheingold, A. L.; Koetzle, T. F. *Acc. Chem. Res.* **1996**, *29*, 348. (b) Shubina, E. S.; Epstein, L. M. *Coord. Chem. Rev.* **2002**, *231*, 165. (c) Custelcean, R.; Jackson, J. S. *Chem. Rev.* **2001**, *101*, 1963. (d) Epstein, L. M.; Belkova, N. V.; Shubina, E. S. In *Recent Advances in Hydride Chemistry*; Peruzzini, M., Poli, R., Eds.; Elsevier: Amsterdam, 2001; Chapter 14, pp 391–418.
- (2) Morris, R. H. In *Recent Advances in Hydride Chemistry*; Peruzzini, M., Poli, R., Eds.; Elsevier: Amsterdam, 2001; Chapter 1, pp 1–38.
- (3) Wessel, E.; Lee, J. C.; Peris, E.; Yap, G. P.; Fortin, J. B.; Ricci, J. S.; Sini, G.; Albinati, A.; Koetzle, T. F.; Eisenstein, O.; Rheingold, A. L.; Crabtree, R. H. *Angew. Chem., Int. Ed. Engl.* **1995**, *34*, 2507.
- (4) Shubina, E. S.; Belkova, N. V.; Krylov, A. N.; Vorontsov, E. V.; Epstein, L. M.; Gusev, D. G.; Niedermann, M.; Berke, H. *J. Am. Chem. Soc.* **1996**, *118*, 1105.
- (5) Ayllón, J. A.; Gervaux, C.; Sabo-Etienne, S.; Chaudret, B. *Organometallics* **1997**, *16*, 2000.

- (6) Shubina, E. S.; Belkova, N. V.; Bakhmutova, E. V.; Vorontsov, E. V.; Bakhmutov, V. I.; Ionidis, A. V.; Bianchini, C.; Marvelli, L.; Peruzzini, M.; Epstein, L. M. *Inorg. Chim. Acta* **1998**, *280*, 302.
- (7) Gruendeman, S.; Ulrich, S.; Limbach, H.-H.; Golubev, N. S.; Denisov, G. S.; Epstein, L. M.; Sabo-Etienne, S.; Chaudret, B. *Inorg. Chem.* **1999**, *38*, 2550.

Scheme 1



Scheme 1. If the cationic dihydrogen complex $[\text{M}-(\eta^2\text{-H}_2)]^+$ is unstable, the alkoxy complex M-OR would be the final product.^{4–6}

In our recent study⁸ of low-temperature (200–250 K) dihydrogen bonding and proton transfer to $\text{CpRuH}(\text{CO})(\text{PCy}_3)$ (**1**) in the low polar media of dichloromethane we have found for the first time experimental evidence of the formation of the hydrogen bond-stabilized ion pair **3**. Moreover, slow interconversion of an $\text{H}\cdots\text{H}$ hydrogen-bonded complex **2a** into a hydrogen-bonded ion pair **3** was shown to be the rate-limiting step of the proton transfer reaction and was followed in the case of PFTB at 200 K. However in dichloromethane at temperatures above 220 K both hydrogen-bonded ion pair **3** and free cationic dihydrogen complex **4** easily lose dihydrogen, producing alkoxycomplexes **6**.

The role of homoconjugate ions ($[\text{X}\cdots\text{H}\cdots\text{X}]^{\text{or}\pm}$) in organic chemistry is well known. Recently its importance in the protonation equilibria has been recognized for organometallic systems.^{9,10} Norton et al.⁹ have justified that the protonation of $\text{CpHW}(\text{CO})_2\text{PMe}_3$ by PhNH_3^+ occurs despite the weak acidic character of PhNH_3^+ because of homoconjugate pair formation between PhNH_3^+ and its conjugate base PhNH_2 . The production of $[\text{PhNH}_2\cdots\text{H}\cdots\text{H}_2\text{NPh}]^+$ has been considered the driving force of the protonation reaction. In our previous study of the protonation of **1** by TFA we pointed out that the dissociation of the ionic pair **3** into the free cationic complex **4** is assisted by the formation of homoconjugate ions $[\text{RO}\cdots\text{H}\cdots\text{OR}]^-$ (**5**).⁸ Such organic complexes with symmetric or quasi-symmetric ionic hydrogen bonds are known as the most stable species in solution whose features have been studied.¹¹

The first computational study on dihydrogen bonding appeared almost simultaneously to the experimental ones,¹² and since then, dihydrogen bonding attracts considerable attention of theoreticians.¹³ The nature and geometrical and energetic features of dihydrogen-bonded complexes have been thoroughly studied. In the very recent work of Alkorta et al.¹⁴ the influence of proton donor strength on structural, energetic, and IR spectroscopic properties of model $\text{X-H}\cdots\text{H-M}$ ($\text{M} = \text{Li}, \text{Na}$) complexes was studied. Nevertheless the role of dihydrogen-bonded complexes as intermediates in protonation reaction is

considered only in a few theoretical works.^{15–17} Modeling the protonation of $\text{CpRuH}(\text{CO})(\text{PH}_3)$ by H_2O , CF_3OH , and H_3O^+ , Scheiner et al.¹⁶ obtained dihydrogen-bonded or nonclassical ($\eta^2\text{-H}_2$) cationic complexes depending on the proton donor strength. The critical role of proton donor acidity was lately recognized by Lau et al.,¹⁷ but to our knowledge there is no work where the roles of solvent and of homoconjugate anion complexes have been taken into account for transition metal hydride protonation, although they have been extensively studied for organic systems.¹⁸

Here we treat the influence of media polarity on the proton transfer to **1** both experimentally and theoretically. The use of nonpolar hexane instead of low-polar dichloromethane in the IR study increases the stability of all species, allowing us to look deeper into the mechanism of proton transfer to hydrides. The results of the kinetic study in hexane utilizing a wider temperature (200–250 K) and concentration range (in comparison to our previous study⁸) presented in this paper gave for the first time the activation enthalpy and entropy of conversion of the $\text{H}\cdots\text{H}$ bonded complex **2** into the ion pair **3** and revealed very interesting peculiarities of this proton transfer process in nonpolar media. Introduction of solvent effects into DFT calculations showed the stabilizing role of solvent in the protonation process and explained the experimental findings. Calculation of the protonation reaction with participation of dimeric $(\text{ROH})_2$ species demonstrates the role played by homoconjugate pairs stabilizing the protonation products.

Experimental Section

The hydride $\text{CpRuH}(\text{CO})\text{PCy}_3$ (**1**) studied in this work was prepared as described.¹⁹ Fluorinated alcohols were from P&M company (Moscow). All manipulations were performed in an atmosphere of dry argon using standard Schlenk techniques. Hexane was dried by refluxing over sodium and distilled under dry argon prior to use. IR measurements were carried out on a “Specord M82” spectrometer in 0.1 cm CaF_2 cells. The study of hydrogen bonds was carried out in the range of XH-stretching vibrations of proton donors in low concentration ($C = 1 \times 10^{-3}$ to 1×10^{-2} mol L^{-1}) in the presence of the hydride excess ($C = 10^{-1}$ to 2×10^{-2} mol L^{-1}). Positions of the band $\nu_{\text{XH}\cdots\text{HRu}}$ correspond to their center of gravity ($s = \pm 3$ cm^{-1}). Studies in the range of stretching vibrations of carbonyl ligands (ν_{CO}) were carried out in the presence of equimolar amounts and of excess of proton donors.

Low-temperature IR measurements were carried out in a Carl Zeiss Jena cryostat in the temperature range 200–300 K using a stream of liquid nitrogen. The accuracy of temperature adjustment was ± 0.5 K. To suppress the reaction, reagents were mixed at low temperatures. Then the cold solution was transferred into the cryostat precooled to a required temperature. The reaction between hydride **1** and PFTB was studied by following the increase of the carbonyl stretch at 1978 cm^{-1} corresponding to hydrogen-bonded ion pair **3**. A representative set of spectral changes is shown in Figure 2. The first-order rates were obtained by plotting $\ln(A_\infty - A_t)$ versus time. Fitting of eq 3 to obtain k_2 and k_{-2} values was done using STATISTICA software²⁰ ($n = 8$, $R = 0.91\text{--}0.97$).

- (8) Belkova, N. V.; Ionidis, A. V.; Epstein, L. M.; Shubina, E. S.; Gruendemann, S.; Golubev, N. S.; Limbach, H.-H. *Eur. J. Inorg. Chem.* **2001**, 1753.
 (9) (a) Papish, E. T.; Rix, F. C.; Spetseris, N.; Norton, J. R.; Williams, R. D. *J. Am. Chem. Soc.* **2000**, *122*, 12235. (b) Papish, E. T.; Magee, M. P.; Norton, J. R. In *Recent Advances in Hydride Chemistry*; Peruzzini, M., Poli, R., Eds.; Elsevier: Amsterdam, 2001; Chapter 2, pp 39–74.
 (10) Fong, T. P.; Forde, C. E.; Lough, A. J.; Morris, R. H.; Rigo, P.; Rocchini, E.; Stephan, T. *J. Chem. Soc., Dalton Trans.* **1999**, 4475.
 (11) (a) Castaneda, J. P.; Denisov, G. S.; Shreiber, V. M. *J. Mol. Struct.* **2001**, *560*, 150. (b) Drichko, N. V.; Kerenskaya, G. I.; Shreiber, V. M. *J. Mol. Structure* **1999**, *304*, 73. (c) Yuchnevich, G. V.; Tarakanova, E. G.; Maiorov, V. D.; Librovich, N. B. *J. Mol. Struct.* **1992**, *265*, 237.
 (12) Liu, Q.; Hoffmann, R. *J. Am. Chem. Soc.* **1995**, *117*, 10108.
 (13) For recent reviews of theoretical work on dihydrogen bonding see: (a) Alkorta, I.; Rozas, I.; Elguero, J. *J. Chem. Soc. Rev.* **1998**, *27*, 163. (b) Maseras, F.; Lledós, A.; Clot, E.; Eisenstein, O. *J. Chem. Soc., Dalton Trans.* **2000**, 615. (c) Clot, E.; Eisenstein, O.; Lee, D. H.; Crabtree, R. H. In *Recent Advances in Hydride Chemistry*; Peruzzini, M., Poli, R., Eds.; Elsevier: Amsterdam, The Netherlands, 2001; Chapter 3, pp 75–88.
 (14) Alkorta, I.; Elguero, J.; Mo, O.; Yañez, M.; Del Bene, J. E. *J. Phys. Chem. A* **2002**, *106*, 9325.

- (15) Orlova, G.; Scheiner, S.; Kar, T. *J. Phys. Chem. A* **1999**, *103*, 514.
 (16) Orlova, G.; Scheiner, S. *J. Phys. Chem. A* **1998**, *102*, 4813.
 (17) Chu, H. S.; Xu, Z.; Ng, S. M.; Lau, C. P.; Lin, Z. *Eur. J. Inorg. Chem.* **2000**, 993.
 (18) Scheiner, S. *Hydrogen Bonding: A Theoretical Perspective*; Oxford University Press: New York, 1997.
 (19) (a) Chinn, M. S.; Heinekey, D. M. *J. Am. Chem. Soc.* **1990**, *112*, 5166. (b) Chinn, M. S.; Heinekey, D. M. *J. Am. Chem. Soc.* **1987**, *109*, 5865.

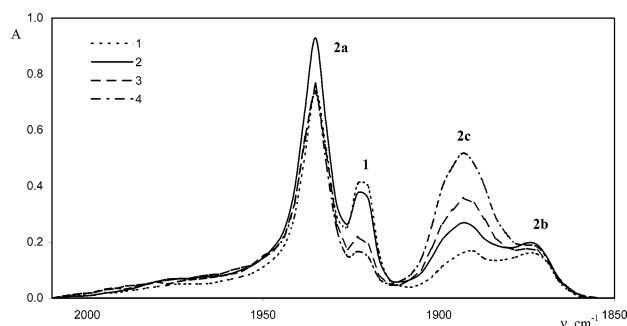


Figure 1. IR spectra in the ν_{CO} range of CpRuH(CO)(PCy₃) (**1**) (0.004 mol L⁻¹) in the presence of excess PFTB at 220 K in hexane; ratio **1**/PFTB = 1:6 (**1**), 1:8 (**2**), 1:12 (**3**), 1:16 (**4**).

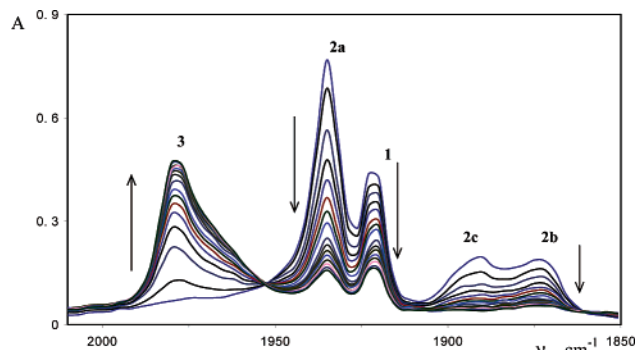


Figure 2. Time-dependent IR spectra in the ν_{CO} range of CpRuH(CO)(PCy₃) (**1**) (0.004 mol L⁻¹) in the presence of 6 equiv of PFTB at 220 K in hexane (over 30 min period).

Computational Details

Calculations were performed with the Gaussian 98 series of programs.²¹ Density functional theory (DFT) was applied with the B3LYP functional.²² Effective core potentials (ECPs) were used to represent the innermost electrons of the ruthenium atom as well as the electron core of phosphorus atom.²³ The basis set for the Ru and P atoms was that associated with the pseudopotential,²³ with a standard double- ζ LANL2DZ contraction,²¹ supplemented in the case of P with a set of d-polarization functions.²⁴ A 6-31G(d,p) basis was used for hydrogen, oxygen, and carbon atoms directly bonded to the metal, while a 6-31G basis set was used for the rest of the atoms in the system.²⁵ Solvent effects were taken into account by means of polarized continuum model (PCM) calculations²⁶ using standard options.²¹ Free energies of solvation were calculated with dichloromethane ($\epsilon = 8.93$)

Table 1. Dependence of IR ν_{CO} Absorptions on Proton Donor Used for Dihydrogen-Bonded Complex **2a**, Ion Pair **3**, and Alkoxy Complex **6**, in Hexane and Dichloromethane^a

HA	$\nu_{\text{CO}}(\mathbf{2a})$, cm ⁻¹	$\nu_{\text{CO}}(\mathbf{3})$, cm ⁻¹	$\nu_{\text{CO}}(\mathbf{4})$, cm ⁻¹	$\nu_{\text{CO}}(\mathbf{6})$, cm ⁻¹
Hexane, $\nu_{\text{CO}}(\mathbf{1}) = 1920$ cm ⁻¹				
HFIP	1931	1972		1946
PFTB	1935	1978		1955
TFA	1940	2004		1963
Dichloromethane, ^a $\nu_{\text{CO}}(\mathbf{1}) = 1890$ cm ⁻¹				
PFTB		1960		1944
TFA		1996	2020	1957
HBF ₄			2020	

^a Data from ref 8.

and *n*-heptane ($\epsilon = 1.92$) as solvents, keeping the geometry optimized for the gas phase species (single-point calculations). For technical reasons, due to the program limitations, it has not been possible to perform calculations in *n*-hexane. However, close values of the dielectric constant were obtained for both solvents ($\epsilon(\text{hexane}) = 2.0$, $\epsilon(\text{heptane}) = 1.92$), suggesting the results for both solvents must be very similar.

Results and Discussion

Hydrogen Bonding and Protonation of **1 in Hexane.** The hydride **1** is of moderate basicity ($E_{\text{J}}^{\text{1d},27} = 1.02$) and forms medium strength ($\Delta H^\circ = -5.1/-7.3$ kcal/mol) hydrogen bonds with fluorinated alcohols.⁸ The values of $\Delta H^\circ = -7.3$ kcal/mol and of $\Delta S^\circ = -21.6$ cal K⁻¹ mol⁻¹ have been determined for the dihydrogen-bonded complex of **1** with PFTB in hexane from the temperature dependence of formation constants K_1 obtained from ν_{CO} intensity changes at 200–250 K.⁸

This hydride exhibits in hexane a quite narrow ($\Delta\nu_{1/2} = 7$ cm⁻¹) band $\nu_{\text{CO}}(\mathbf{1})$ at 1920 cm⁻¹. Upon addition of a proton donor, a new band belonging to the hydrogen-bonded complex **2a** arises immediately at *higher* frequency, which does not overlap with the $\nu_{\text{CO}}(\mathbf{1})$ band. The position of this $\nu_{\text{CO}}(\mathbf{2a})$ band depends on the complex strength: the more stable the hydrogen-bonded complex, the larger the band shift (Table 1).

Studying the interaction of **1** with PFTB at different alcohol concentrations surprisingly we observed another new band $\nu_{\text{CO}}(\mathbf{2b})$ at 1872 cm⁻¹. Such *low-frequency* shift (-48 cm⁻¹) is typical for hydrogen bonding to a carbonyl group,²⁸ and we believe this band belongs to the hydrogen-bonded complex **2b** (Scheme 2). At 6-fold PFTB excess (and higher) another band arises at 1892 cm⁻¹ (Figure 1), which belongs to the hydrogen-bonded complex **2c** between **1** and two PFTB molecules (Scheme 2). This situation is similar to what we observed for the ν_{NO} band of rhenium hydride ReH₂(CO)(NO)(PET₃)₂.²⁹ This hydride formed hydrogen-bonded complexes of ReH \cdots HOR and NO \cdots HOR types, which appeared in the IR spectra as two new bands shifted to higher and lower frequencies relative to the ν_{NO} band of the free hydride. The hydrogen-bonded complex with two alcohol molecules contained both H \cdots H and NO \cdots H bonds, and its ν_{NO} band appeared in the spectra 20 cm⁻¹ higher than the ν_{NO} band in the ReNO \cdots HOR complex.²⁹

(20) STATISTICA for Windows [Computer program manual]; StatSoft, Inc.: Tulsa, OK, 1999.

(21) Frisch, M. J.; Trucks, G. W.; Schlegel, H. B.; Scuseria, G. E.; Robb, M. A.; Cheeseman, J. R.; Zakrzewski, V. G.; Montgomery, J. A., Jr.; Stratmann, R. E.; Burant, J. C.; Dapprich, S.; Millam, J. M.; Daniels, A. D.; Kudin, K. N.; Strain, M. C.; Farkas, O.; Tomasi, J.; Barone, V.; Cossi, M.; Cammi, R.; Mennucci, B.; Pomelli, C.; Adamo, C.; Clifford, S.; Ochterski, J.; Petersson, G. A.; Ayala, P. Y.; Cui, Q.; Morokuma, K.; Malick, D. K.; Rabuck, A. D.; Raghavachari, K.; Foresman, J. B.; Cioslowski, J.; Ortiz, J. V.; Stefanov, B. B.; Liu, G.; Liashenko, A.; Piskorz, P.; Komaromi, I.; Gomperts, R.; Martin, R. L.; Fox, D. J.; Keith, T.; Al-Laham, M. A.; Peng, C. Y.; Nanayakkara, A.; Gonzalez, C.; Challacombe, M.; Gill, P. M. W.; Johnson, B.; Chen, W.; Wong, M. W.; Andres, J. L.; Gonzalez, C.; Head-Gordon, M.; Replogle, E. S.; Pople, J. A. *Gaussian 98*; Gaussian, Inc.: Pittsburgh, PA, 1998.

(22) (a) Lee, C.; Yang, W.; Parr, R. G. *Phys. Rev. B* **1988**, *37*, 785. (b) Becke, A. D. *J. Chem. Phys.* **1993**, *98*, 5648. (c) Stephens, P. J.; Devlin, F. J.; Chabalowski, C. F.; Frisch, M. J. *J. Phys. Chem.* **1994**, *98*, 11623.

(23) (a) Hay, P. J.; Wadt, W. R. *J. Chem. Phys.* **1985**, *82*, 299. (b) Wadt, W. R.; Hay, P. J. *J. Chem. Phys.* **1985**, *82*, 284.

(24) Höllwarth, A.; Böhme, M.; Dapprich, S.; Ehlers, A. W.; Gobbi, A.; Jonas, V.; Köhler, K. F.; Stegmann, R.; Veldkamp, A.; Frenking, G. *Chem. Phys. Lett.* **1993**, *208*, 237.

(25) (a) Francl, M. M.; Pietro, W. J.; Hehre, W. J.; Binkley, J. S.; Gordon, M. S.; Defrees, D. J.; Pople, J. A. *J. Chem. Phys.* **1982**, *77*, 3654. (b) Hehre, W. J.; Ditchfield, R.; Pople, J. A. *J. Chem. Phys.* **1972**, *56*, 2257. (c) Hariharan, P. C.; Pople, J. A. *Theor. Chim. Acta* **1973**, *28*, 213.

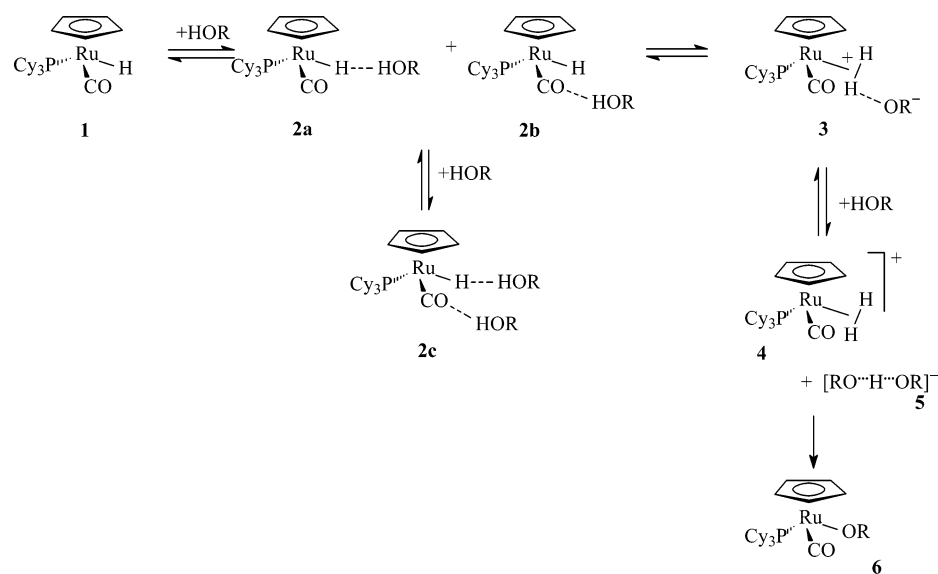
(26) (a) Tomasi, J.; Persico, M. *Chem. Rev.* **1994**, *94*, 2027. (b) Amovilli, C.; Barone, V.; Cammi, R.; Cancès, E.; Cossi, M.; Mennucci, B.; Pomelli, C. S.; Tomasi, J. *Adv. Quantum Chem.* **1998**, *32*, 227.

(27) Iogansen, A. V. *Theor. Experim. Khim.* **1971**, 302–320.

(28) (a) Kazarian, S. G.; Hamley, P. A.; Poliakov, M. *J. Chem. Soc., Chem. Commun.* **1992**, 994. (b) Kazarian, S. G.; Hamley, P. A.; Poliakov, M. *J. Am. Chem. Soc.* **1993**, *115*, 9069. (c) Hamley, P. A.; Kazarian, S. G.; Poliakov, M. *Organometallics* **1994**, *13*, 1767.

(29) Belkova, N. V.; Shubina, E. S.; Gutsul, E. I.; Epstein, L. M.; Nefedov, S. E.; Eremenko, I. L. *Inorg. Chim. Acta* **2000**, *610*, 58.

Scheme 2



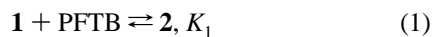
Similarly to the situation in dichloromethane,⁸ the interaction does not stop at this point and all the ν_{CO} bands of the hydrogen-bonded complexes decrease in time, while the high-frequency ν_{CO} band of the hydrogen-bonded ion pair **3** appears and grows (Figure 2). The position of the ν_{CO} (**3**) band depends on the nature of the proton donor used. As can be seen from the data in Table 1, a weaker proton donor having a more basic conjugated anion produces a larger low-frequency shift from the position of the ν_{CO} (**4**) band of the free cationic dihydrogen complex, which can be associated with a stronger hydrogen-bonding interaction within the corresponding ion pair: TFA < PFTB < HFIP.

The strength of the proton donor determines not only the strength of the hydrogen-bonding interaction in **2** and **3** but also the protonation reaction rate and the time of the equilibrium **2** \leftrightarrow **3** settlement. While the formation of ion pair **3** by the reaction of **1** with TFA at 200 K proceeds almost immediately, it takes about 1 h in the case of PFTB and even longer (3–4 h) in the case of HFIP at the same temperature. So, we concentrated our efforts on studying the kinetics of proton transfer from **2** to **3** in hexane using PFTB as a proton donor, which gives reaction rates optimal for measurement by conventional IR techniques with some freedom to change the reaction conditions such as temperature and concentration of the reagents.

Kinetics of Proton Transfer in Hexane. We studied the kinetics of protonation of **1** by PFTB at 200–240 K (with 10 K steps); concentrations used were 0.003–0.010 mol/L for **1** and 0.006–0.080 mol/L for the alcohol.

Despite the diversity of hydrogen-bonded species, the proton transfer process in Scheme 2 can be simplified into two consecutive equilibrium steps: **1** + PFTB \rightleftharpoons **2** \rightleftharpoons **3**. From the kinetic point of view this represents a typical reaction with so-called rapid preequilibrium.

diffusion-controlled first stage:



rate-limiting step:



We studied the kinetics of this reaction following the intensity

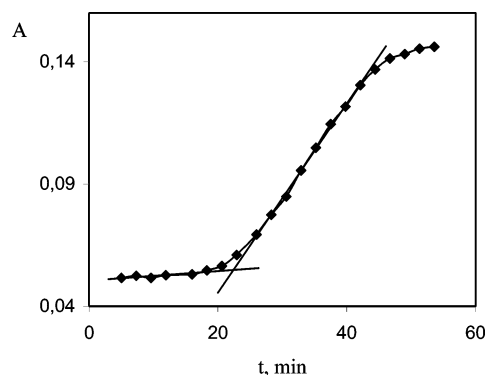


Figure 3. Kinetic curve for the reaction of CpRuH(CO)(PCy₃) (**1**) (0.004 mol L⁻¹) with 2 equiv of PFTB at 240 K in hexane.

changes of the ν_{CO} (**3**) band, which gave the same results as ν_{CO} (**1**) and ν_{CO} (**2a**).

Unexpectedly we found that at low alcohol concentration an induction period t_{ind} exists, as one can see from the representative kinetic curve in Figure 3. This induction period t_{ind} (determined as depicted in Figure 3) gets shorter with the increase of PFTB concentration and almost disappears at 6-fold alcohol excess at 220 K (Figure 4a). Moreover the increase of total concentrations of reagents (from 0.003 to 0.004 and 0.005 mol/L of **1** at 240 K) keeping the hydride–PFTB ratio at 1:5 leads to disappearance of the induction period, as does a temperature increase.

The observed rate constants k_{obs} were determined from the plots of $\ln(A_{\infty} - A_t)$ versus time considering only the part of the kinetic curve after the induction period. It appeared that k_{obs} becomes independent of PFTB concentration at the same concentration as t_{ind} disappears (Figure 4b).

The explanation of this phenomenon can be proposed on the basis of the comparison of the hexane and dichloromethane properties. The rather polar medium, in which proton transfer is usually studied, preferentially stabilizes the ion pair, causing proton transfer toward the base.¹⁸ Dichloromethane is indeed a rather polar solvent, whose dielectric constant increases dramatically by lowering the temperature.⁷ Dichloromethane molecules easily create a polar shell around the hydrogen-bonded complex,

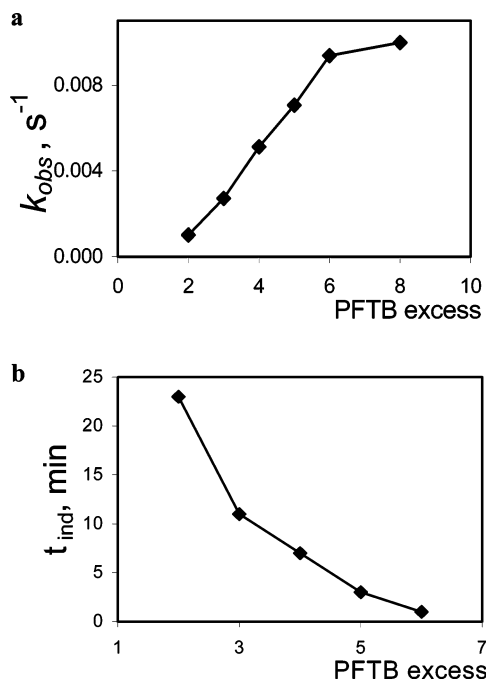


Figure 4. Influence of alcohol concentration on the induction period t_{ind} (a) and rate constant k_{obs} (b) for the reaction of CpRuH(CO)(PCy₃) (**1**) (0.004 mol L⁻¹) with PFTB at 220 K in hexane.

which assists proton transfer by increasing local polarity.³⁰ In the case of nonpolar solvents such as hexane the oriented polarization of the solvent molecules assists proton transfer impossible in the gas phase.³¹ In addition, we suppose that the orientation of the alcohol molecules can take place increasing the shell polarity around the hydrogen-bonded complex. At low proton donor concentrations such organization probably takes some time, being the cause of the existence of the induction period.

The observed rate constant in the present case can be described by eq 3.

$$k_{\text{obs}} = k_2 \left(\frac{K_1[\text{HA}]}{1 + K_1[\text{HA}]} \right) + k_{-2} \quad (3)$$

Fitting this equation gives real values for the k_2 and k_{-2} rate constants, which are 5.4×10^{-2} and 1.1×10^{-3} s⁻¹, respectively, at 240 K. Correspondingly, the equilibrium constant $K_2 = k_2/k_{-2}$ (eq 2) is equal to 49. Unfortunately at lower temperatures we observed that the reaction does not reach equilibrium. Instead at some point the intensity of the ν_{CO} (**3**) band decreases probably due to the low solubility and the precipitation of the ion-paired complex **3**. This fact precluded us from determining K_2 values at other temperatures. Nevertheless, we were able to estimate k_2 values taking into account that k_{-2} is at least 2 orders of magnitude less than k_2 and can be neglected. So, obtained in this way the k_2 values range from 5.4×10^{-2} s⁻¹ at 240 K to 4.5×10^{-4} s⁻¹ at 200 K. These data allow us to use the Eyring plot (Figure 5) and calculate (eq 4) for the first time the enthalpy and entropy of activation for proton transfer from the dihydrogen-bonded complex to the (η^2 -H₂)-complex: $\Delta H^\ddagger = 11.0 \pm 0.5$ kcal/mol and $\Delta S^\ddagger = -19 \pm 3$ eu.

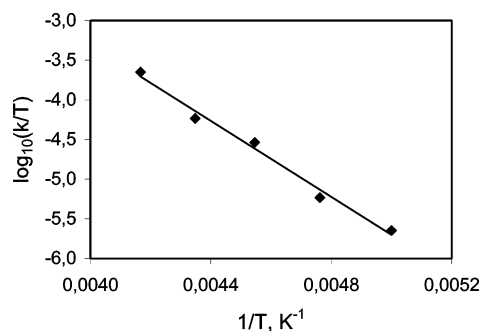


Figure 5. Eyring plot of $\log(k_2/T)$ vs $1/T$ for transformation of CpRu(CO)(PCy₃)H \cdots HOC(CF₃)₃ (**2a**) into [CpRu(CO)(PCy₃)(η^2 -H₂)]⁺ \cdots ⁻OC(CF₃)₃ (**3**).

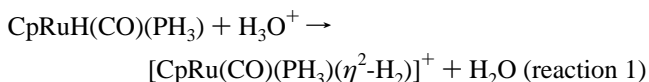
$$\log(k_2/T) = -\frac{\Delta H^\ddagger}{4.576T} + \frac{\Delta S^\ddagger}{4.576} + 10.319 \quad (4)$$

The free energy of activation of the proton transfer ΔG^\ddagger at 200 K is slightly higher in hexane (14.8 kcal/mol) than in dichloromethane (14.1 kcal/mol),⁸ in agreement with theoretical findings (see below). The major difference observed when moving from dichloromethane to hexane solvents is the decrease in the stability of the dihydrogen-anion ion pair (found both experimentally and theoretically) and the increase of the energy barrier in the charge separation process, shown theoretically.

Theoretical Study of the Proton Transfer. The large amount of experimental data accumulated for the protonation of CpRuH(CO)(PR₃) complexes makes them a very good target to perform a theoretical study of the factors governing the transition metal-hydride protonation. First of all we will present the results for the bimolecular reaction in the gas phase and we will analyze further how they are modified when solvent effect and homo-conjugate pairs are taken into account.

Proton Transfer in the Gas Phase. We have considered the interaction of CpRuH(CO)(PH₃) (**1t**) with H₃O⁺, CF₃COOH (TFA), and (CF₃)₃COH (PFTB) as proton donors of different strength. As several structures had been calculated in the theoretical study of Orlova and Scheiner,¹⁶ this preliminary study will also serve to evaluate our methodology.

When the strong acid H₃O⁺ is placed near **1t**, a proton transfer to the hydride takes place without barrier and the dihydrogen complex [CpRu(CO)(PH₃)(η^2 -H₂)]⁺ (**4t**) is formed. The optimized geometries of **1t** and **4t** are depicted in Figure 6. In agreement with the previous study no dihydrogen-bonded intermediate is found. It is known that **1** forms a stable cationic dihydrogen complex under the action of HBF₄.¹⁹ The same result was obtained for the complex CpRuH(CO)(PⁱPr₃).³² Although the presence of traces of the *trans*-dihydrido isomer have been reported,³² it was found 3.5 kcal/mol less stable than **1t** in the previous study, and we have not considered it. The reaction



is very exothermic. Products are found 48.1 kcal/mol below reactants.

(30) Golubev, N. S.; Schenderovich, I. G.; Smirnov, S. N.; Denisov, G. S.; Limbach, H.-H. *Chem. Eur. J.* **1999**, *5*, 492

(31) Denisov, G. S.; Kulbida, A. I.; Mikheev, V. A.; Rumynskaya, I. G.; Shreiber, V. M. *J. Mol. Liq.* **1983**, *26*, 159.

(32) Esteruelas, M. A.; Gómez, A. V.; Lahoz, F. J.; López, A. M.; Oñate, E.; Oro, L. A. *Organometallics* **1996**, *15*, 3423.

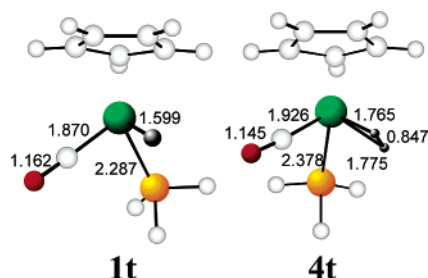


Figure 6. Optimized geometries of CpRuH(CO)(PH₃) (**1t**) and [CpRu(CO)(PH₃)(η²-H₂)]⁺ (**4t**).

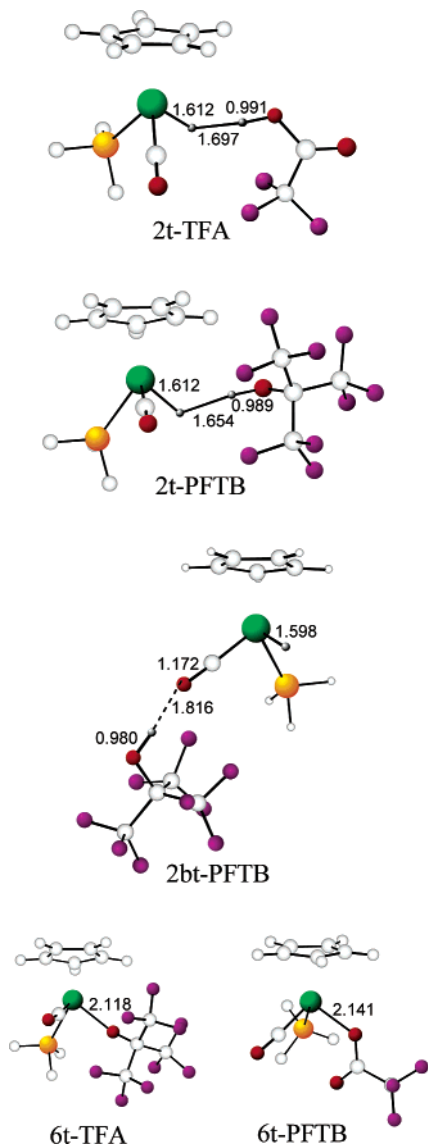


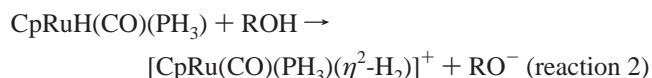
Figure 7. Optimized geometries of CpRuH(CO)(PH₃)...CF₃COOH (**2t-TFA**), CpRuH(CO)(PH₃)...CF₃COH (**2t-PFTB**), CpRuH(PH₃)(CO)...CF₃COH (**2bt-PFTB**), CpRu(CO)(PH₃)(OCOCF₃) (**6t-TFA**), and CpRu(CO)(PH₃)(OC(CF₃)₃) (**6t-PFTB**).

When weaker proton donors such as TFA and PFTB are placed near **1t**, the optimization leads to the dihydrogen-bonded complexes **2t-TFA** and **2t-PFTB**, respectively. Both complexes present similar geometries, shown in Figure 7. The formation of the hydrogen bond between the hydride and the proton is reflected in the lengthening of the Ru-H and O-H bond distances from their values in the isolated compounds (Ru-H,

1.599 Å in **1t**; O-H, 0.972 Å in TFA and 0.971 Å in PFTB). Our structures compare well with that previously reported for CF₃OH.¹⁶ The thermodynamics of the dihydrogen bond formation with both proton donors is similar. In the gas phase, Δ*E* values of -8.4 and -9.7 kcal/mol are found for TFA and PFTB, respectively. These values compare well with calculated values reported in the literature for this kind of interaction.^{1,13} However, our calculated value for PFTB is higher than the experimental value of **1** in hexane (Δ*H*^o = -7.3 kcal/mol).

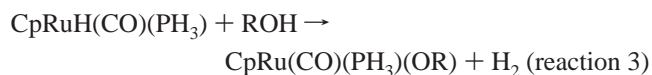
We have also considered the possibility of formation of a CO...HOR hydrogen bond. Starting the optimization with a PFTB molecule in the carbonyl region, we have obtained the structure **2bt-PFTB** (Figure 7), which corresponds to the proposed hydrogen-bonded complex **2b**. The formation of the hydrogen bond involving the carbonyl ligand is reflected in the lengthening of the CO bond distance from its value in **1t** (1.172 Å in **2bt-PFTB**, 1.162 Å in **1t**). The binding energy of this CO...HOR hydrogen bond (-8.4 kcal/mol) indicates that it is of similar strength to the MH...HOR dihydrogen bond and thus that the carbonyl and hydrogen ligands can compete as hydrogen bond acceptor sites.

Our results indicate that in the case of poor or moderate proton donors, a dihydrogen-bonded intermediate is initially formed in the protonation pathway. In the next step, proton transfer from ROH to CpRuH(CO)(PH₃) should lead to the formation of the ionic pair [CpRu(CO)(PH₃)(η²-H₂)]⁺...OR⁻. We have searched for this minimum, but all attempts to find it ended up in the dihydrogen-bonded complexes **2t-TFA** and **2t-PFTB**. Thus, in the gas phase the conjugate OR⁻ bases are so strong that they pull the proton from the dihydrogen complex and no minimum like **3** is found. Considering the cationic dihydrogen complex and the anion infinitely apart we have calculated the thermodynamics of the proton transfer reaction:



As expected, due to the net charge creation in the reaction (neutral reactants and +1 and -1 products), this process is extremely unfavorable in the gas phase. Products are found 107.7 kcal/mol (for CF₃COOH) and 111.5 kcal/mol (for (CF₃)₃-COH) above the reactants.

It has been observed that at temperatures above 220 K **4** loses a dihydrogen molecule and alkoxy complexes **6** are produced. The protonation of similar hydride CpRuH(CO)(PⁱPr₃) with HBF₄ in acetone leads to [CpRu(η¹-OC(CH₃)₂)(CO)(PⁱPr₃)]⁺ by releasing H₂.³² We have optimized the geometries of the complexes CpRu(CO)(PH₃)(OCOCF₃) (**6t-TFA**) and CpRu(CO)(PH₃)(OC(CF₃)₃) (**6t-PFTB**) (Figure 7). The feasibility of the dihydrogen elimination can be appreciated looking at the thermodynamics of the reaction



Products are found 6.8 kcal/mol below the reactants for ROH = TFA and 2.7 kcal/mol above for ROH = PFTB.

Gas phase results show the dependence of the proton transfer to a metal hydride on the proton donor strength.¹⁶ For a strong proton donor there is no energy barrier for the protonation, whereas moderate proton donors form complexes of H...H

bonding type, but are unable to overcome the huge barrier required for the formation of the dihydrogen complex **3** in the gas phase. In the next section we will show how solvent assists the proton transfer.

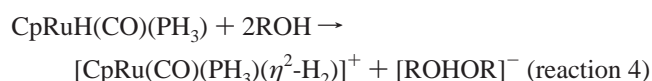
Solvent Effects. We have calculated the thermodynamics of reaction 1 in *n*-heptane and dichloromethane. Both solvents stabilize preferentially the smallest charged species (H₃O⁺), leading to a decrease of the exothermicity. In *n*-heptane products are found 26.6 kcal/mol below the reactants, and in the more polar dichloromethane 13.6 kcal/mol below the reactants.

We have performed solvent calculations for all the species found in the gas phase study with TFA and PFTB proton donors. Formation energies of the dihydrogen-bonded species change only slightly when the solvent is taken into account, but in all cases the interaction energy between the transition metal hydride and the proton donor decreases when the polarity of the solvent increases. Values of −5.2 and −2.4 kcal/mol have been obtained for **2t-TFA** in *n*-heptane and dichloromethane, respectively. For **2t-PFTB** the calculated values are −5.6 kcal/mol in heptane and −2.4 kcal/mol in dichloromethane. The calculated value for **2t-PFTB** in heptane is in reasonable agreement with the experimental value in hexane ($\Delta H^\circ = -7.3$ kcal/mol). Thus, theoretical values obtained in the gas phase overestimated the strength of the H⋯H interaction. The binding energies for the CO⋯HOR hydrogen-bonded complex **2bt-PFTB** in heptane and dichloromethane are −4.9 and −3.2 kcal/mol, respectively. These solution values do support the coexistence of the dihydrogen-bonded complex **2a** with the hydrogen-bonded complex **2b**, as suggested by the IR study (Figure 1).

As expected, polar solvents stabilize charged species, and the strongest effect introduced by the solvent is on the relative stabilities of the charged species **4t** and OR[−]. The thermodynamics of reaction 2 is dramatically changed. **4t** + CF₃COO[−] are found 64.6 and 22.1 kcal/mol above the reactants, in heptane and dichloromethane, respectively. Values for **4t** + (CF₃)₃CO[−] are 72.5 kcal/mol (heptane) and 32.1 kcal/mol (dichloromethane). We must point out that even considering the strongest proton donor (TFA) and the more polar solvent (dichloromethane), the solvent-separated ions are still 22.1 kcal/mol above the reactants. With this result, we cannot account for the observation of dihydrogen complexes in solution.

Given the electroneutrality of reaction 3, solvent effects are not very important for this process. The stability of the products slightly decreases increasing the solvent polarity. **6t-TFA** lies 5.5 kcal/mol below the reactants in heptane and 4.2 kcal/mol in dichloromethane. **6t-PFTB** is found 6.0 and 8.1 kcal/mol above the reactants, in heptane and dichloromethane, respectively.

Role of Homoconjugate Anionic Species [ROHOR][−]. To investigate the possibility that homoconjugate ions play a role in the protonation, we have theoretically studied the proton transfer reaction with participation of two ROH molecules of the proton donor, both in the gas phase and in solution. After the proton transfer takes place a [ROHOR][−] anion will be present in the media. The overall reaction is



CF₃COOH As Proton Donor. There are multiple possibilities for hydrogen bonding in a system with the metal hydride **1**

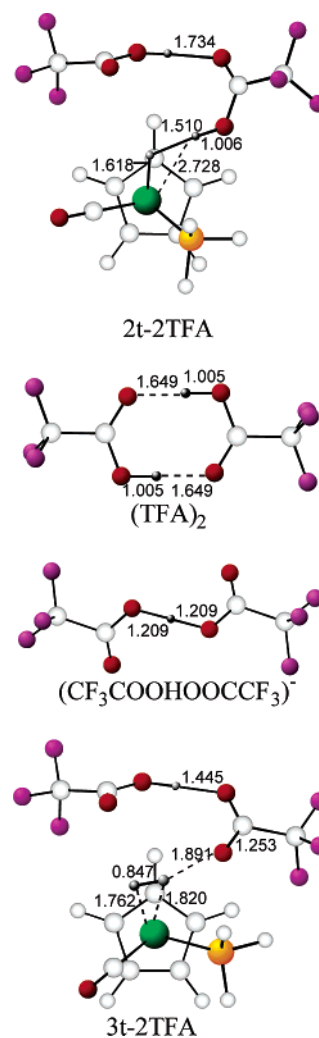


Figure 8. Optimized geometries of CpRuH(CO)(PH₃)⋯(CF₃COOH)₂ (**2t-2TFA**), (CF₃COOH)₂, [CpRu(CO)(PH₃)(η²-H₂)]⁺⋯[CF₃COOHOOCCF₃][−] (**3t-2TFA**), and [CF₃COOHOOCCF₃][−].

and two molecules of TFA. As we are interested in [ROHOR][−] anion formation, we have not performed a systematic search of all the minima, but we have taken as a starting point the optimized geometry of **2t-TFA** and placed a new molecule of the acid forming a hydrogen bond with the carbonylic oxygen of the former. In this way we have found the dihydrogen-bonded complex **2t-2TFA**, in which H⋯H and O⋯H hydrogen bonds are present (Figure 8a). An energy scheme with the relative energies of all the species involved in the proton transfer with the TFA dimer is depicted in Figure 9. The zero of energy in this figure corresponds to the hydride **1t**, with two CF₃COOH molecules infinitely apart. The dihydrogen-bonded complex is found 24.5 kcal/mol below the reactants. The extra stabilization with respect to the monomer case is due to the hydrogen bond between the two TFA molecules. If **1t** with the (CF₃COOH)₂ dimer is taken as the origin of energies, the interaction energy is only 1.7 kcal/mol. This low value comes from the destabilization introduced by the rupture of one strong O—H⋯O interaction, present in the bifurcated dimer (Figure 8b), which is in part compensated by the new Ru—H⋯H—O interaction.

One important point when considering the dimeric species is that now the ion pair **3**, formed by the cationic dihydrogen complex and the anion, is found as a minimum, even in the gas

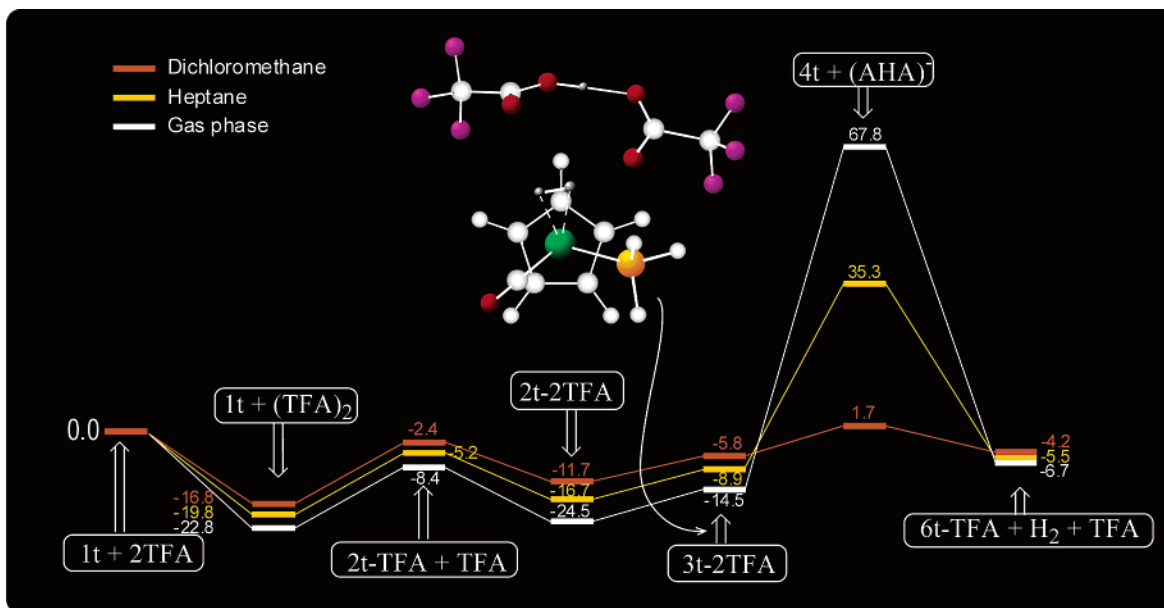


Figure 9. Energy scheme of the protonation of **1t** with $(\text{CF}_3\text{COOH})_2$. Energies are in kcal/mol.

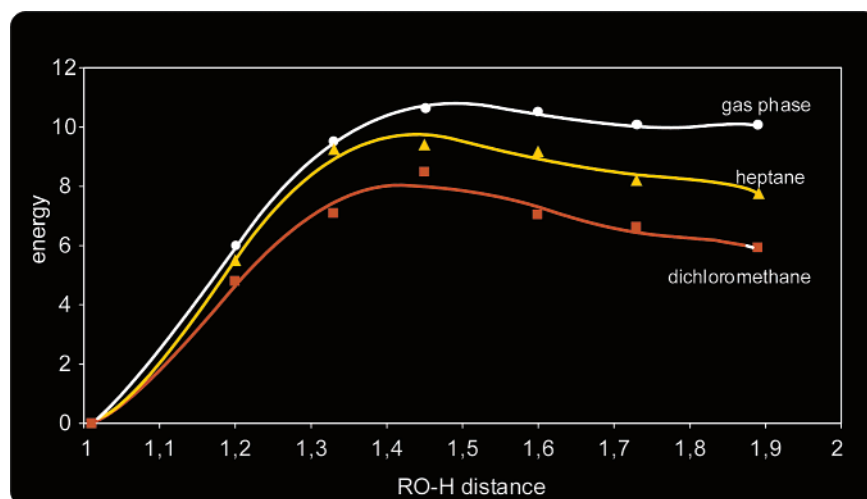


Figure 10. Potential energy curves for the $2t\text{-2TFA} \rightarrow 3t\text{-2TFA}$ process taking the O–H distance of the transferring proton as a reaction coordinate. Energies are in kcal/mol.

phase. Starting from **4t** and $(\text{CF}_3\text{COO}\cdots\text{H}\cdots\text{OOC}\text{CF}_3)^-$ the optimization does not revert to the dihydrogen-bonded complex **2t-2TFA**, but it ends up in the ion pair **3t-2TFA** (Figure 8). In this intermediate the $\eta^2\text{-H}_2$ acts as a hydrogen bond donor to the electronegative atom of the incoming base RO^- . For the first time such an intermediate in the proton transfer pathway between a moderate proton donor and a neutral hydride has been obtained in a theoretical study, thus supporting the experimental evidence of this kind of intermediate.⁸ A hydrogen bond between the dihydrogen ligand and the oxygen of the anion is at work, stabilizing this ion pair complex. As a consequence of the hydrogen bond, the Ru–H distances of the dihydrogen ligand are not equivalent, and the dihydrogen is tilted. We can see in Figure 9 that **3t-2TFA** is found only 10 kcal/mol above the reactant complex **2t-2TFA**. In gas phase calculations the presence of $[\text{ROHOR}]^-$ stabilizes the dihydrogen. The reduced basicity of $[\text{ROHOR}]^-$ in front of that of RO^- prevents pulling out a proton from the dihydrogen complex and allows it to be a stable species. However, even with the introduction of an

additional TFA molecule the charge separation process, which leads from the ion pair to solvent-separated ions, is extremely unfavorable. Solvent will play a major role in this step.

We have calculated the energies of all the species involved in the proton transfer between **1t** and a dimer of TFA in heptane and dichloromethane. Solvent effects are minor for neutral species. When increasing solvent polarity, both the dihydrogen-bonded complex and the ion pair are destabilized with respect to the separated reactants (Figure 9). However solvent effects play a minor role in the dihydrogen-bonded complex/ion pair equilibrium. The thermodynamics of the proton transfer step (energy difference between **3t-TFA** and **2t-TFA**) are not very much affected by the solvent. The ion pair is 10 kcal/mol above the dihydrogen-bonded complex in the gas phase, 7.8 kcal/mol above in heptane, and 5.9 kcal/mol in dichloromethane. On the contrary, the solvent polarity is crucial in the charge separation process, from the ion pair to the solvent-separated ions. Solvents of low dielectric constant, like hexane and dichloromethane, will favor the formation of ion pairs. On the contrary, in solvents

of high dielectric constant most of the ions will be solvent-separated and not ion-paired.

The formation of the $[\text{RO}\cdots\text{H}\cdots\text{OR}]^-$, with a strong hydrogen bond (Figure 8), stabilizes the solvent-separated ions and displaces the equilibrium in reaction 2 toward the products. When both the formation of the homoconjugate anion complex and the solvent effects are taken into account, the protonation of the ruthenium metal hydride by a moderate proton donor such as TFA becomes feasible. As can be seen in Figure 9, the process in dichloromethane exhibits a very smooth energy profile. The highest energy species (the solvent-separated ions) lies only 1.7 kcal/mol above the separated reactants. A considerably slower charge separation is predicted in heptane, as experimental data in hexane indicate. Our theoretical study confirms the proposal that the formation of homoconjugate pairs can be the driving force for the protonation of transition metal hydrides by weak acids.

Until now we have considered only the thermodynamics of the proton transfer. We will focus now on the kinetic aspects. As no transition states are expected either for the process of formation of a dihydrogen-bonded complex or for the charge separation process, we have considered only the proton transfer step. To estimate the energy barrier for this step, we have computed the potential energy curve for the $2\mathbf{t}\text{-}2\mathbf{TFA} \rightarrow 3\mathbf{t}\text{-}2\mathbf{TFA}$ process, taking the O–H distance of the transferring proton as a reaction coordinate and optimizing all the geometrical parameters at each fixed value of this distance. The O–H distance varies from 1.000 Å in the dihydrogen-bonded hydride to 1.891 Å in the dihydrogen cation. The potential energy curves in the gas phase, *n*-heptane, and dichloromethane are depicted in Figure 10, taking as zero energy that of each dihydrogen-bonded complex **2**. The energy profiles present a low barrier, in agreement with the fast process observed for the formation of an ion pair by reaction of **1** with TFA. Increasing the media polarity decreases slightly the barrier, and the lowest barrier is found for the reaction in dichloromethane. A slightly larger stabilization due to solvent effect is found for the ion pair than for the dihydrogen-bonded hydride. This factor makes the barrier for the reverse reaction (deprotonation of the dihydrogen) increase when the media polarity increases. In fact this reaction has almost no barrier in the gas phase, in agreement with the difficulties encountered in locating a stable dihydrogen complex–anion ion pair.

(CF₃)₃COH As Proton Donor. We have performed the same calculations described above with (CF₃)₃COH as proton donor. Calculated structures are depicted in Figure 11, and an energy scheme of the whole process is shown in Figure 12. We first optimized the dihydrogen-bonded species $2\mathbf{t}\text{-}2\mathbf{PFTB}$ (Figure 11). As in the previous case, we did not perform a search for several hydrogen-bonded minima, but we added a PFTB molecule to the optimized structure of the monomer, with the O–H bond of the second molecule interacting with the O of the former. The main difference with TFA is that now the same oxygen atom is involved in the two hydrogen bonds. The relative energy of the $2\mathbf{t}\text{-}2\mathbf{PFTB}$ complex with respect to the monomer case reflects the extra stabilization caused by the additional hydrogen bond.

We have also considered the formation of a species such as **2c**, in which one molecule of PFTB is forming a dihydrogen bond with the hydride while a second molecule of PFTB is

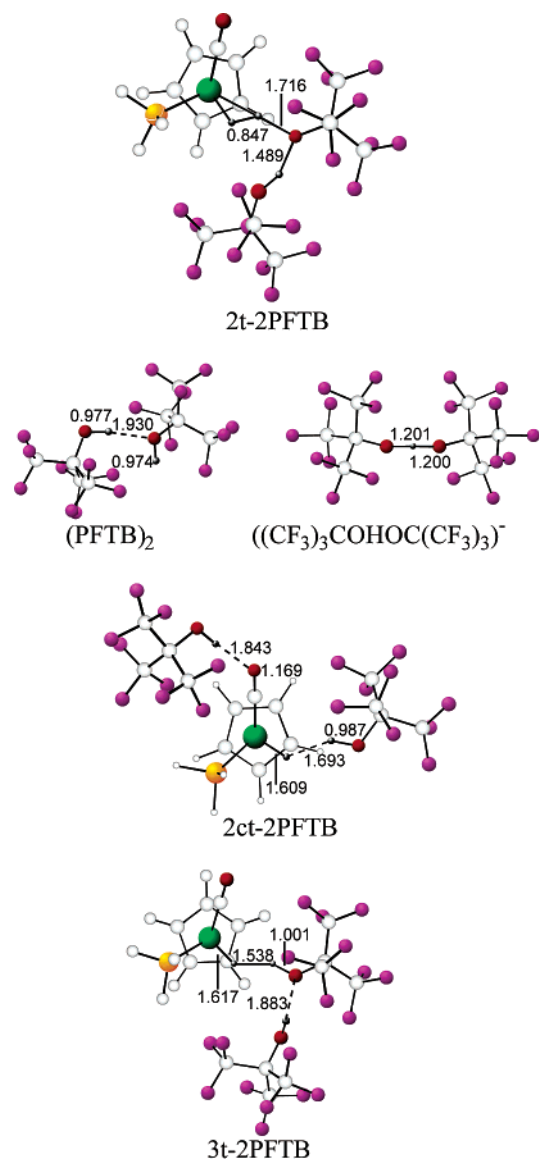


Figure 11. Optimized geometries of CpRuH(CO)(PH₃) \cdots ((CF₃)₃COH)₂ (**2t-2PFTB**), ((CF₃)₃COH)₂ (**2PFTB**), CpRuH(CO) \cdots HOC(CF₃)₃(PH₃) \cdots (CF₃)₃COH (**2ct-2PFTB**), [CpRu(CO)(PH₃)(η^2 -H₂)]⁺ \cdots [(CF₃)₃COHOC(CF₃)₃]⁻ (**3t-2PFTB**), and [(CF₃)₃COHOC(CF₃)₃]⁻.

forming a hydrogen bond with the carbonylic oxygen atom. The optimized structure of this adduct (**2ct-2PFTB**) is given in Figure 11. Comparing the relative energies of this adduct in the gas phase, heptane, and dichloromethane (−17.6, −7.8, and −2.5 kcal/mol, respectively) with the same values for **2t-2PFTB** (−19.6, −7.7, and −1.9 kcal/mol, see Figure 12), it is clear that the hydroxylic oxygen of the dihydrogen-bonded PFTB molecule and the carbonylic oxygen of the CO ligand are competing as hydrogen-bonding acceptors for the proton of the second PFTB molecule. This result accounts for the experimental detection of **2c** at 6-fold and higher PFTB excess.

We have not been able to locate a minimum structure corresponding to the ion pair minimum **3t-PFTB** in the gas phase. This result can be explained looking at the gas phase energy profile for TFA (Figure 10). With a less strong acid such as PFTB (a stronger conjugated base) it can be expected that the reverse reaction occurs without barrier, thus giving rise to only a minimum (**2t-PFTB**). To estimate the energy of the ion

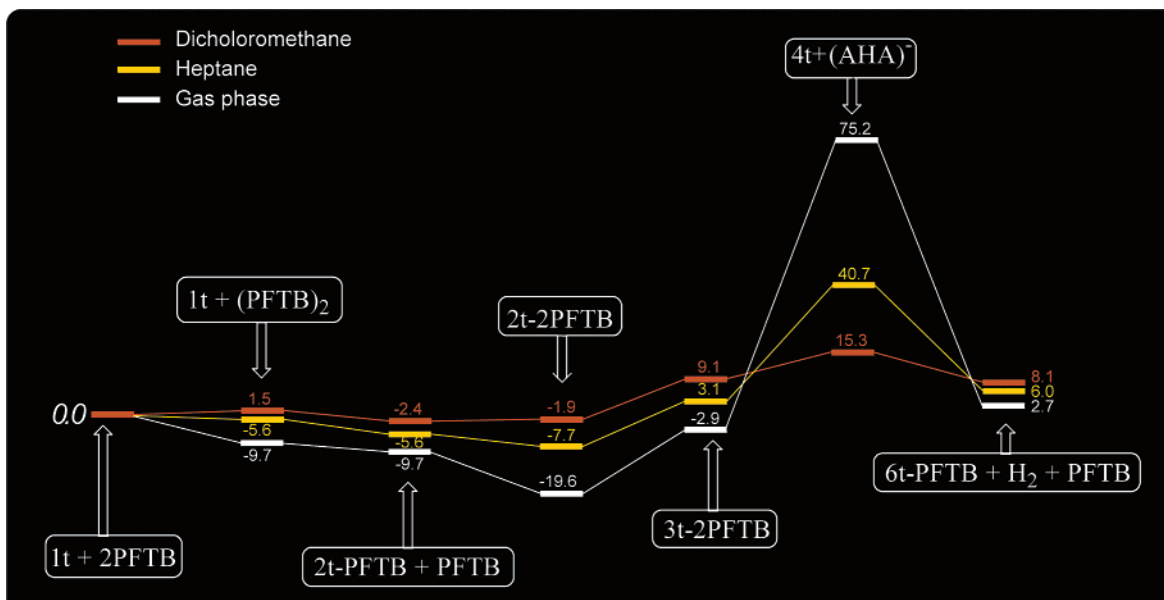


Figure 12. Energy scheme of the protonation of **1t** with $((CF_3)_3COH)_2$. Energies are in kcal/mol.

pair and to get a structure to perform calculations in solvent, we have optimized the structure of the ion pair with the dihydrogen H–H distance and the Ru–H–H angle fixed at the values we obtained for **3t-2TFA** (0.847 Å and 80.2°, respectively). This structure, depicted in Figure 11, is found 4.5 kcal/mol above **1t** + $((CF_3)_3COH)_2$ (Figure 12).

Solvent effects are not very important for the relative stabilities of the dihydrogen-bonded and the ion pair species. In all cases both species are destabilized with respect to separated reactants. It is worth mentioning the interaction energy calculated for the $(CF_3)_3COH$ dimer in dichloromethane. Its positive value (+1.5 kcal/mol) nicely shows that our calculations are able to reproduce that this alcohol is not susceptible to self-association. An interesting point is the energy of the proton transfer step (**2t-2PFTB** → **3t-2PFTB**). The process is endothermic, with energy differences of 16.7, 10.8, and 11.0 kcal/mol in the gas phase, *n*-heptane, and dichloromethane, respectively. We have seen for TFA that the energy barrier for the proton transfer is very small and that the energy differences are not very far from the potential energy barriers (Figure 10). So, our calculated energy difference for the proton transfer in heptane with PFTB as a proton donor (10.8 kcal/mol) is in good agreement with the experimentally determined ΔH^\ddagger (11.0 ± 0.5 kcal/mol). The calculated values for PFTB are considerably higher than those for TFA, in agreement with slower proton transfer.

Given the low dielectric constant of the solvents we are using, the charge separation step to obtain solvent-separated ions appears as a difficult process, in the same way as that for TFA. Energy differences between the ion pair **3t-2PFTB** and the solvent-separated ions are similar to those obtained for TFA. However for PFTB all the species from the dihydrogen-bonded complex to the alkoxy product are found between 5 and 15 kcal/mol higher than for TFA.

Conclusion

Despite its apparent simplicity, the protonation of a transition metal hydride appears as a complicated process in which hydride basicity, proton donor strength, solvent polarity, secondary

interactions among the acids and bases present, and concentration effects are relevant. The hydride ligand of the CpRuH-(CO)(PR₃) complexes is basic enough to be protonated not only by strong acids but also by moderate ones, offering the possibility of analyzing all the factors that play a role in the hydride protonation. With this in mind we used the combination of the low-temperature IR study and DFT calculations. In DFT calculations the proton transfer process was studied both in the gas phase and in low-polar media. The solvent nature and homoconjugate anion effects were taken into account for the first time. The protonation with a strong acid takes place without barrier, and only the cationic dihydrogen complex or products of the dihydrogen elimination are obtained. In this case increasing the solvent polarity decreases the exothermicity of the reaction.

The spectral and theoretical studies of proton transfer with moderate or weak acids show a double-well energy surface. The two minima are the dihydrogen-bonded hydride-proton complex (**2**) and the ion pair stabilized by hydrogen bonds between the dihydrogen ligand and the anion (**3**), and they are separated by an energy barrier that depends on the proton donor strength and the solvent. The stability of the hydrogen-bonded ion pair **3** increases with the counteranion basicity. Moreover, it is possible to achieve a fine-tuning of the thermodynamics and kinetics of the **2** to **3** transformation by means of the dielectric constant of the solvent and the capability of the proton donor to form homoconjugate pairs.

The DFT calculations also show the critical role of the solvent polarity in the stability of the hydrogen-bonded ion pairs and in the increase of the energy barrier in the charge separation process, in agreement with the experimental finding. The use of nonpolar hexane in the IR experiments really increases the stability of all the species, allowing us to look deeper into the mechanism of proton transfer to hydrides. Very interesting peculiarities of the proton transfer process in nonpolar media were revealed, such as the competition between hydride ligand and CO groups as the additional site of hydrogen bonding, the existence of an induction period at low concentration of the

proton donor, and the higher activation barrier than in CH₂Cl₂. The results of the kinetic study gave for the first time the activation enthalpy and entropy of conversion of M–H···H–OR hydrogen-bonded complex **2** into a [M–(η²-H₂)]⁺···OR⁻ ion pair **3**. The computed values of the activation energy are in very good agreement with those values.

A methodological conclusion arises from this paper: despite the complexity inherent to the theoretical modeling of solution processes, it is not always necessary to go to very complex methods to represent the reactive media, as long as the key interactions are included in the calculations. A combined experimental and theoretical study of the hydrogen bonding to OsHCl(CO)(P^tBu₂Me)₂ demonstrated the importance of the proper modeling of the system when studying this kind of problem.³³ In our studied systems the numerical values would be more precise and slightly different if more ROH molecules would be included, but the agreement with the experimental

data we have attained indicates that the essential part of the interactions is already represented with only two ROH molecules and including the solvent effects with a continuum model.

Acknowledgment. Thanks are expressed to Prof. H.-H. Limbach for fruitful discussions. This work was supported by Russian Foundation for Basic Research (02-03-32194, 02-03-06380), INTAS (00-00179), and the Spanish “Dirección General de Investigación” (Project BQU2002-04110-CO2-02). The use of computational facilities of the Centre de Supercomputació de Catalunya (C⁴) is gratefully appreciated. Partial support from the EC-RTN project “Hydrochem” (HPRN-CT-2002-00176) is also acknowledged.

Supporting Information Available: Tables of the optimized geometries (Cartesian coordinates) for all the calculated species. This material is available free of charge via the Internet at <http://pubs.acs.org>.

JA029712A

(33) Yandulov, D. V.; Caulton, K. G.; Belkova, N. V.; Shubina, E. S.; Epstein, L. M.; Khoroshun, D. V.; Musaev, D. G.; Morokuma, K. *J. Am. Chem. Soc.* **1998**, *120*, 12553.